MECHANISMS OF ASTROPHYSICAL JET FORMATION, AND COMPARISON WITH LABORATORY EXPERIMENTS

G.S. Bisnovatyi-Kogan

Space Research Institute of Rus. Acad. Sci., Moscow, Russia
and
National Research Nuclear University MEPhI, Moscow, Russia

TOPICAL PROBLEMS OF
NONLINEAR WAVE PHYSICS
WORKSHOP LaB
July 25, 2017

First model of AGN & quasar, as supermassive black hole, surrounded by accretion disk

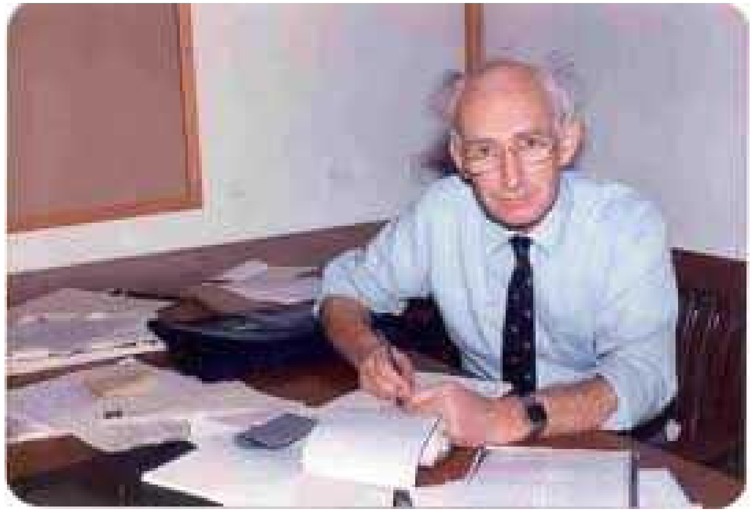

1. Lynden-Bell, D. Galactic Nuclei as Collapsed Old Quasars. Nature, Volume 223, Issue 5207, pp. 690-694 (1969).

Quasars and AGN contain supermassive black holes

About 10 HMXR - stellar mass black holes in the Galaxy: microquasars.

Jets are observed in objects with black holes: collimated ejection from accretion disks.

Non-relativistic jets are observed in young stellar-like objects

Jet in M87:

radio, 14GHz, **VLA,** 0.2”

HST (F814W)

Chandra image, 0.2”, 0.2-8 keV

Adaptively smoothed **Chandra** image

From

Marshall et al. (2001)

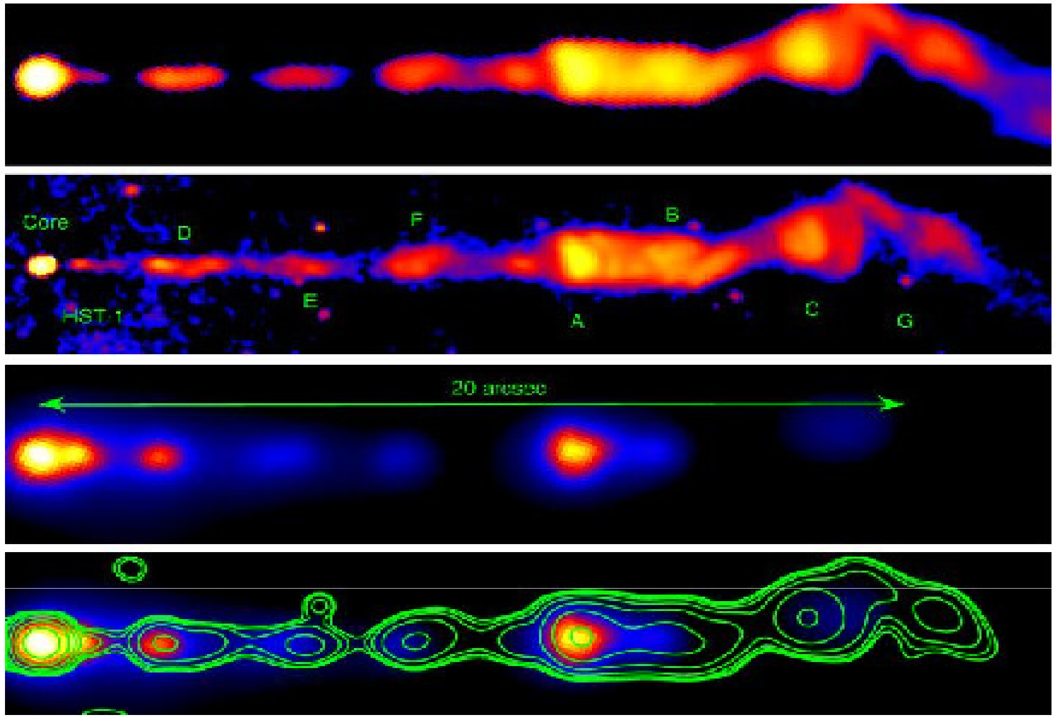

Fig. 1.— Images of the jet in M 87 in three different bands, rotated to be horizontal, and an overlay of optical contours over the X-ray image. *Top:* Image at 14.435 GHz using the VLA. The spatial resolution is about 0.2″. *Second panel:* The *Hubble* Space Telescope Planetary Camera image in the F814W filter from Perlman et al. (2001a). The brightest knots are labelled according to the nomenclature used by Perlman et al. (2001a) and others. *Third panel:* Adaptively smoothed *Chandra* image of the X-ray emission from the jet of M 87 in 0.20″ pixels. The X-ray and optical images have been registered to each other to about 0.05″ using the position of the core. *Fourth panel:* Smoothed *Chandra* image overlaid with contours of a Gaussian smoothed version of the HST image, designed to match the *Chandra* point response function. The X-ray and optical images have been registered to each other to about 0.05″ using the position of the core. The HST and VLA images are displayed using a logarithmic stretch to bring out faint features while the X-ray image scaling is linear.

3C 273

Left:

MERLIN, 1.647 GHz.

Middle:

HST(F622W), 6170A.

Right:

Chandra, 0.1 “

Marshall et al. (2000)

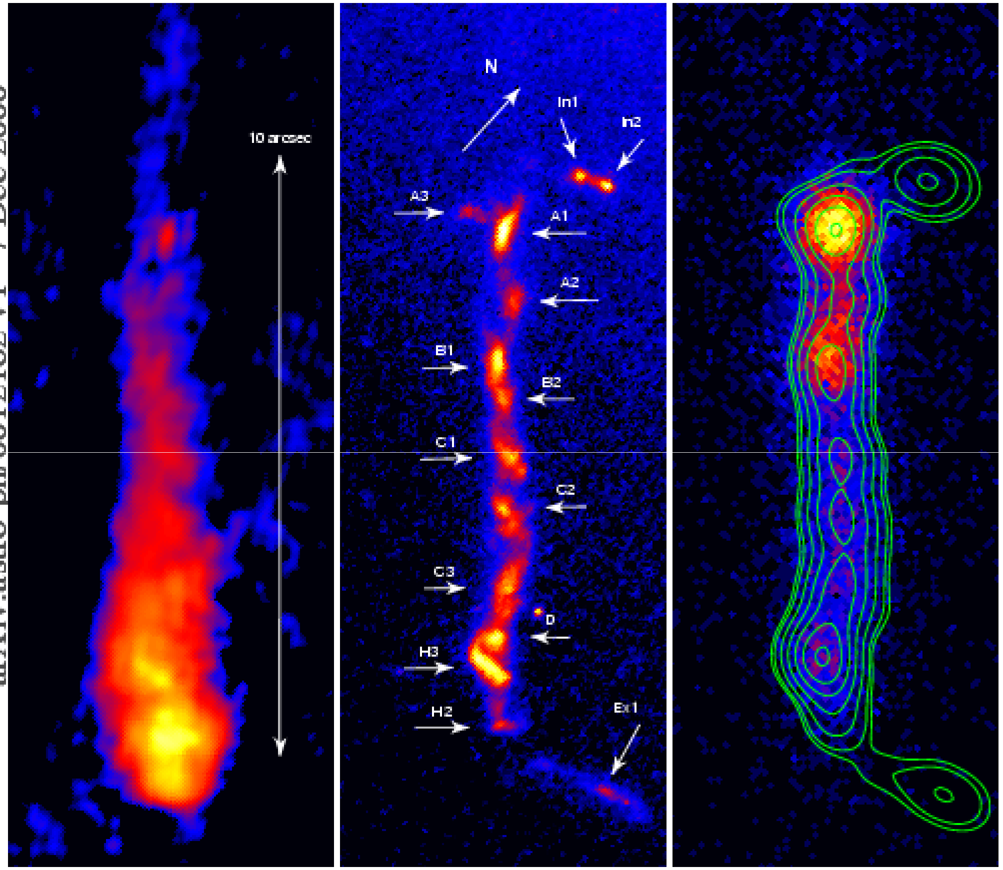

Jet in radiogalaxy

IC 4296 at 20 cm with 3.2” resolution.

10” is about 2 kps.

VLA, Killeen et al. (1986)

Total extent is about

400 kpc

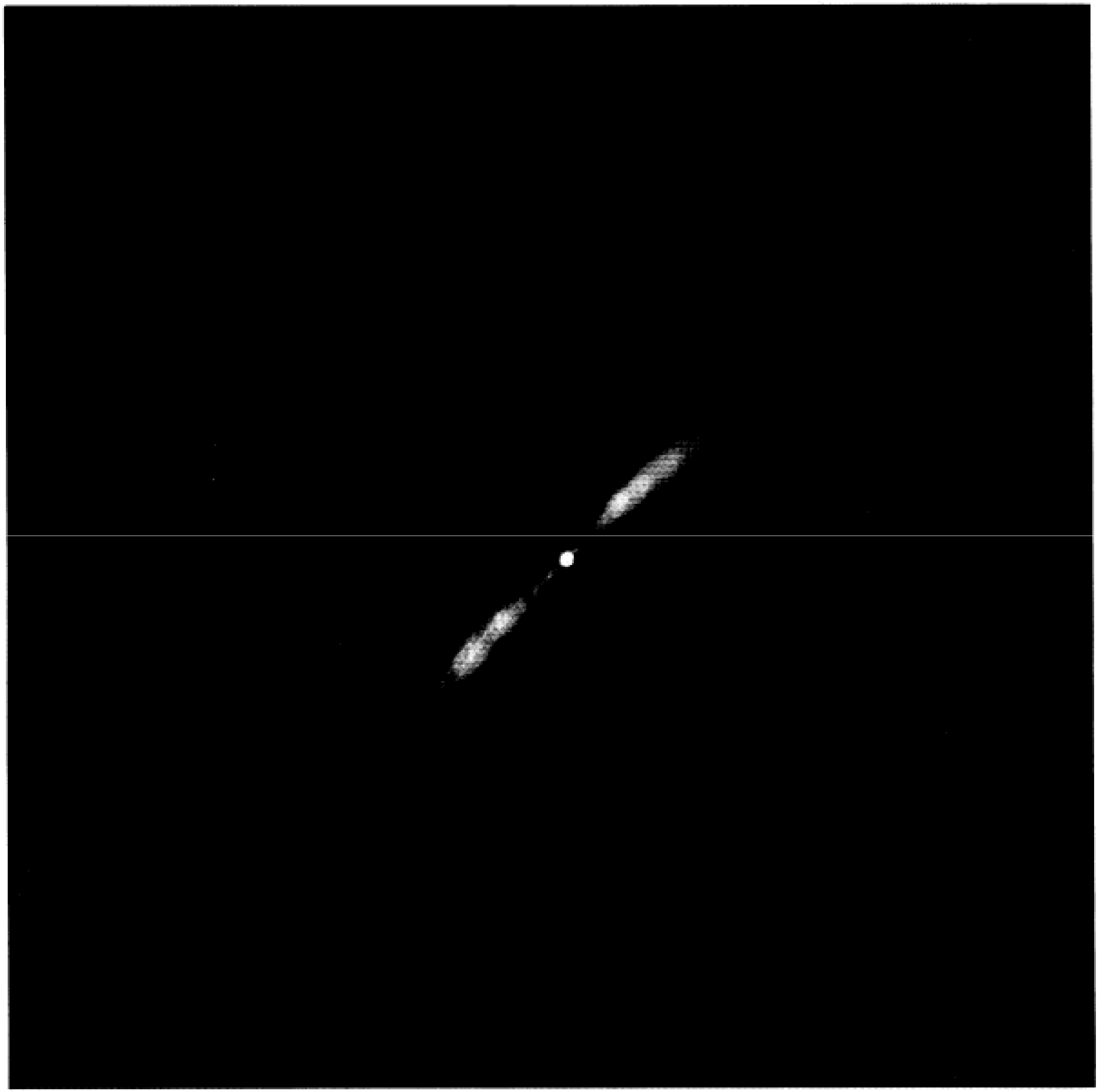

FIG. 11.—Radiograph of the jets at 20 cm with 3."2 resolution

KILLEEN (*see* page 311)

Microquasar

GRS 1915+105

Jet ejection

MERLIN 5GHz

Fender (1999)

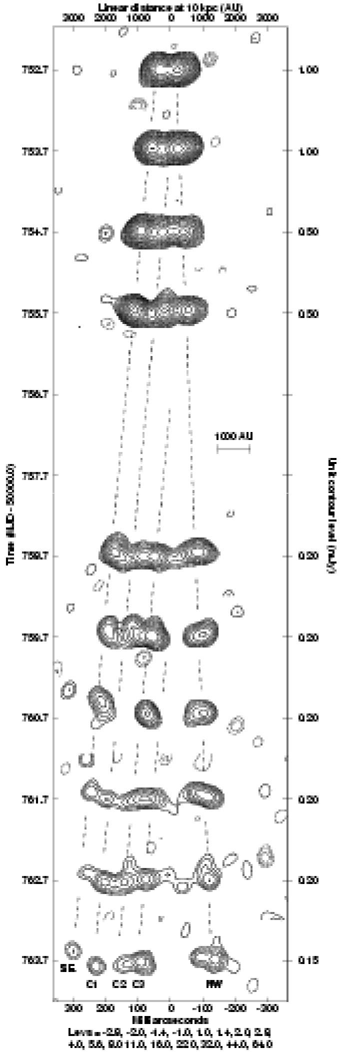

Fig. 2. A sequence of ten epochs of radio imaging of relativistic ejections from the black hole candidate X-ray binary GRS 1915+105 using MERLIN at 5 GHz. The figure has been rotated by 52 degrees to form the montage. Contour levels increase in factors of $\sqrt{2}$ from the unit contour level indicated at the right hand side of each image. Components SE, C1, C2 & C3 are approaching with a mean proper motion of 23.6 ± 0.5 mas d^{-1}. Component NW is receding with a mean proper motion of 10.0 ± 0.5 mas d^{-1} and corresponds to the same ejection event which produced approaching component SE. For an estimated distance to the source of 11 kpc the approaching components have an apparent transverse velocity of 1.5c. Assuming an intrinsically symmetric ejection and the standard model for apparent superluminal motions, we derive an intrinsic bulk velocity for the ejecta of $0.98^{+0.02}_{-0.05}c$ at an angle to the line of sight of 66 ± 2 degrees (at 11 kpc). The ejections occurred after a 20-day 'plateau' during which the X-ray emission was hard and stable and the radio had an inverted spectrum. The first two ejections were punctuated by four days of rapid radio oscillations, indicative of an unstable inner accretion disc being repeatedly ejected [14,38,34,8,16]. The apparent curvature of the jet is probably real, although the cause of the bending is uncertain. A detailed presentation and discussion of these results may be found in [18].

THE ACCRETION OF MATTER BY A COLLAPSING STAR IN THE PRESENCE OF A MAGNETIC FIELD

G. S. BISNOVATYI-KOGAN and A. A. RUZMAIKIN

Institute of Applied Mathematics, U.S.S.R. Academy of Sciences, Moscow, U.S.S.R.

(Received June 27, 1973)

Astrophysics and Space Science **28** (1974) 45–59.

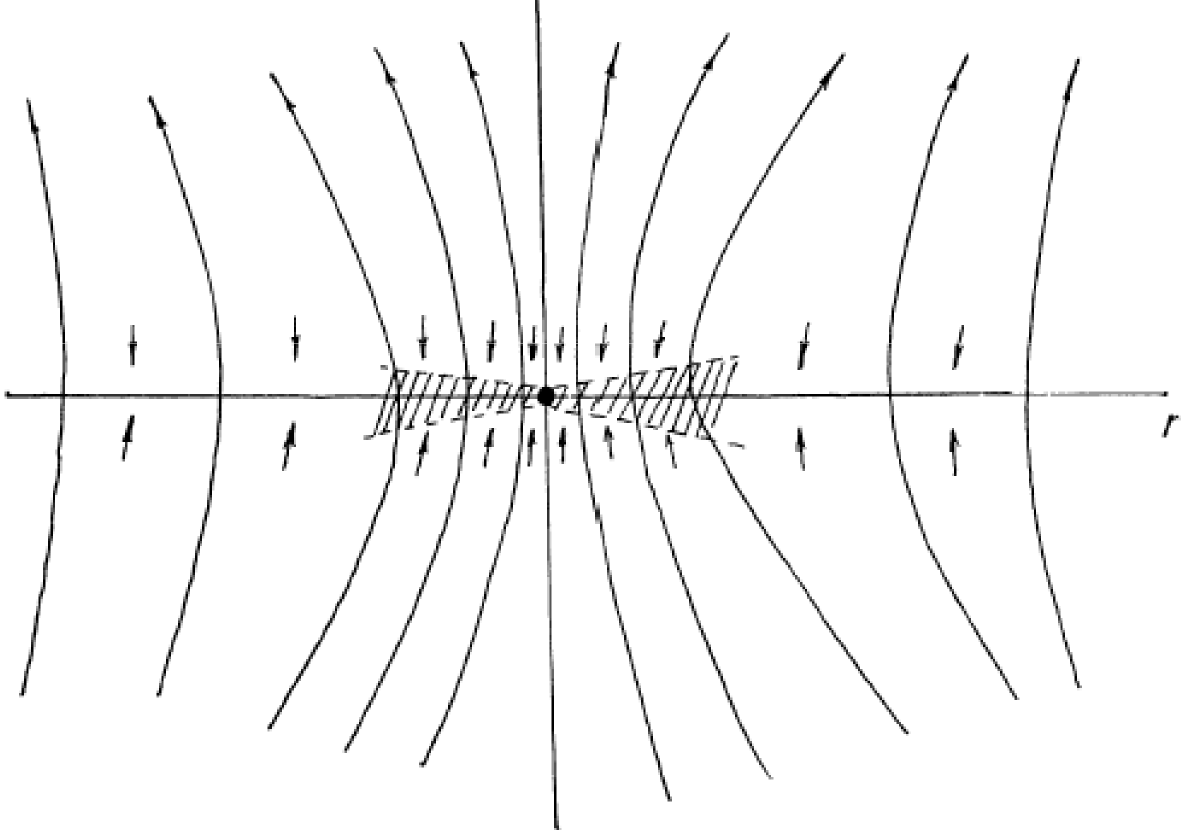

Fig. 1. A qualitative picture of the accretion of matter on to a c.s. with a frozen, regular magnetic field. Arrows indicate the direction of motion of the matter. The magnetic field far from the star lies in the direction of the z-axis and its sense is indicated by arrows on the lines of force. The infalling matter forms a disk in the plane $\theta = \pi/2$, which slowly settles to the star. In the flow region $E_B \sim E_{\rm kin}$, and rotation is entirely absent.

THE ACCRETION OF MATTER BY A COLLAPSING STAR
IN THE PRESENCE OF A MAGNETIC FIELD.
II. SELFCONSISTENT STATIONARY PICTURE

G. S. BISNOVATYI-KOGAN
Space Research Institute, U.S.S.R. Academy of Science, Moscow, U.S.S.R.
and
A. A. RUZMAIKIN
Institute of Applied Mathematics, U.S.S.R. Academy of Science, Moscow, U.S.S.R.

(Received 26 August, 1975)

Astrophysics and Space Science **42** (1976) 401–424.

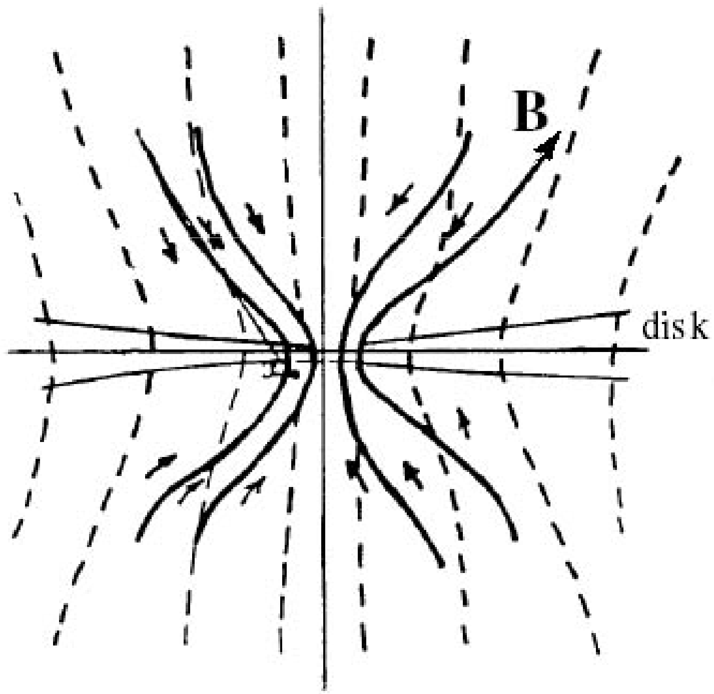

Sketch of the magnetic field threading an accretion disk.
Shown increase of the field owing to flux freezing in the accreting disk matter

At presence of large-scale magnetic field the efficiency of accretion is always large (0.3-0.5) of the rest mass energy flux

Accretion disk around BH with large scale magnetic field (non-rotating disk)

Turbulent electrical conductivity, analog of alpha viscosity

$$\sigma_t = \frac{c^2}{\tilde{\alpha} 4\pi h \sqrt{P/\varrho}},$$

$10^7 – 10^{10}$ Gs in the vicinity of a black hole

“alpha disk” model

$$t_{\varphi r} = \alpha P$$

$t_{\varphi r}$ – viscous stress

P – pressure

Algebraic relation

(Shakura 1972)

Angular velocity gradient dependent viscous stress

$$t_{\varphi r} = \rho \nu r \frac{d\Omega}{dr}, \qquad \nu = \alpha \rho u_{s0} z_0$$

ν – kinematic viscosity coefficient

ρ – density

Ω – angular velocity

A hot corona around a black-hole accretion disk as a model for Cygnus X-1

G. S. Bisnovatyi-Kogan and S. I. Blinnikov

Institute for Space Research, USSR Academy of Sciences, Moscow

(Submitted April 15, 1976) Sov.Astron.Lett. 2, 191-193 (Sep.-Oct. 1976)

Mechanism for producing fast particles which is analogous to the pulsar process. If magnetized matter with low angular momentum falls into the black hole (in addition to the disk accretion), a strong poloidal magnetic field will arise . By analogy to pulsars, rotation will generate an electric field of strength $E \approx -(v/c)B$ in which electrons are accelerated to energies Energy $\approx R(v/c)B\, e \approx 3 \cdot 10^4$ [B/(10^7 Gauss)] Mev where $v/c \approx 0.1$ and $R \approx 10^7$ cm is the characteristic scale. In a field $B \approx 10^7$ Gauss, such electrons will generate synchrotron radiation with energies up to $\approx 10^5$ keV. It would be possible here for e^+e^- pairs to be formed and to participate in the synchrotron radiation.

Sketch of picture of a disk accretion on to a black hole
at sub-critical luminosity.

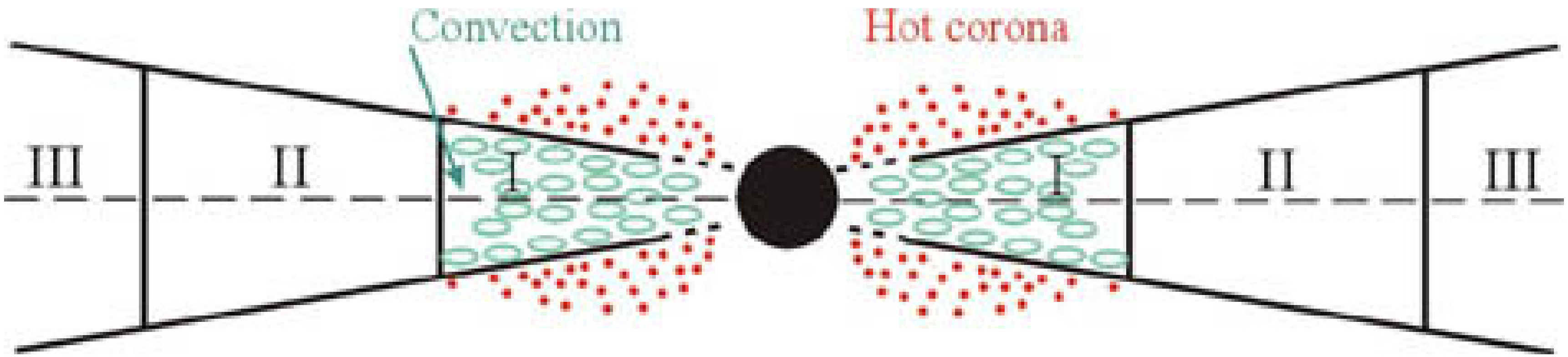

I – radiation dominated region, electron scattering.
II – gas-dominated region, electron scattering.
III- gas-dominated region, Krammers opacity.

Dynamo model of double radio sources

Lovelace, R. V. E.

Nature, vol. 262, Aug. 19, 1976, p. 649-652.

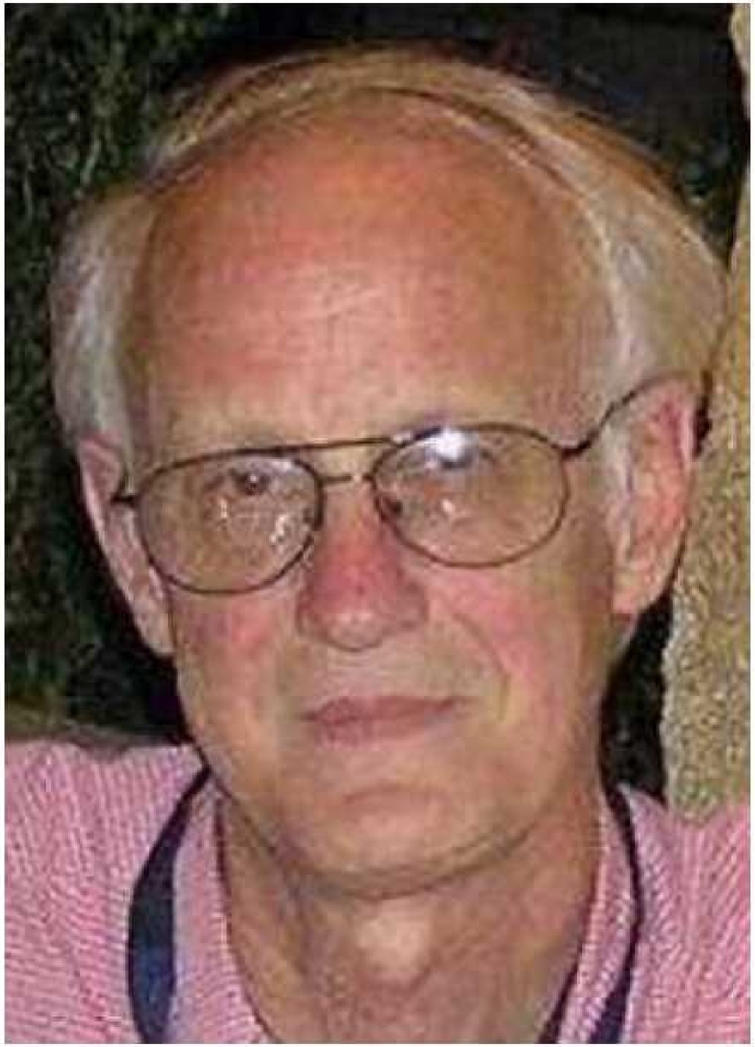

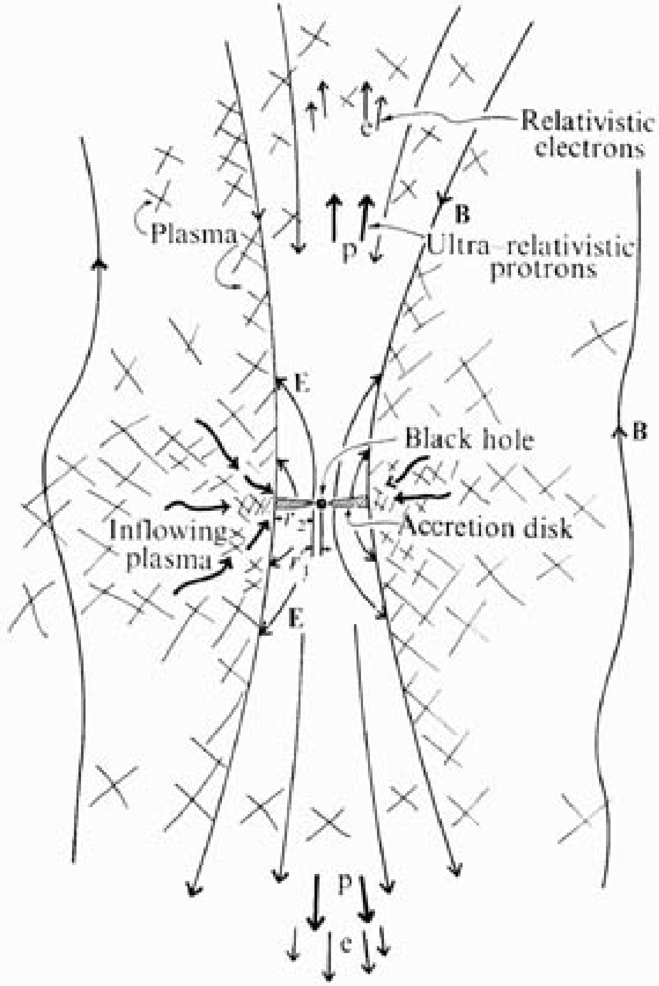

Jet formation in the accretion disk around BH (sketch)

Set of equations for “αP” viscosity prescription with advection

Optically thick-thin transition

$$
\begin{cases}
r\dfrac{v'}{v} = \dfrac{N}{D} \\[2ex]
r\dfrac{c_s'}{c_s} = \left(1 - \dfrac{v^2}{c^2}\right)\dfrac{N}{D} + 1 - r\dfrac{\Omega_K'}{\Omega_K} + \dfrac{\Omega^2 - \Omega_K^2}{c_s^2} r^2 \\[2ex]
\Omega = \dfrac{l_{in}}{r^2} + \alpha\dfrac{c_s^2}{vr}
\end{cases}
$$

Artemova Yu. V.
Bisnovatyi-Kogan G. S.
Igumenshchev I. V.
Novikov I. D.
ApJ, 2006, 637:968–977

where $\left(\,'\,\right) \equiv \dfrac{d}{dr}$

N, D - functions of $r, \Omega, \Omega_K, \beta, v, c_s, l_{in}, \alpha, \dot{M}$

$$
\beta = \frac{P_g}{P}, \quad (1-\beta)P = \frac{aT_c^4}{3}\,\frac{1 + \dfrac{4}{3\tau_0}}{1 + \dfrac{4}{3\tau_0} + \dfrac{2}{3\tau_*^2}}
$$

$$
T = \beta\frac{c_s^2 c^2}{R}
$$

A.S. Klepnev and G. S. Bisnovatyi-Kogan

Astrophysics, Vol. 53, No. 3, p. 409-418, 2010

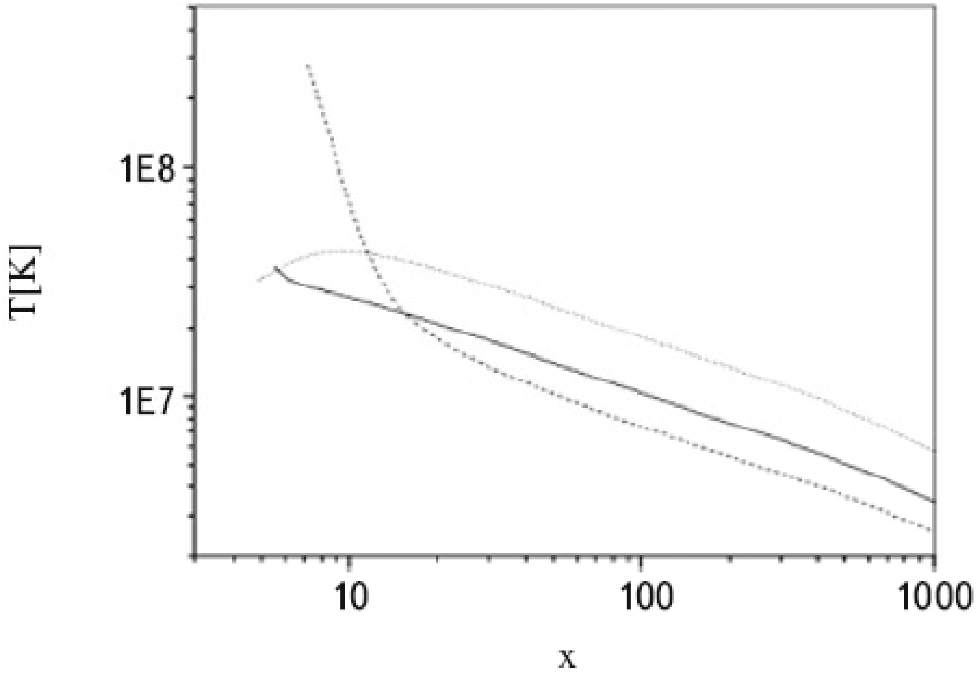

Fig. 3. The radial dependence of the temperature of the accretion disk for an accretion rate $\dot{m} = 50$ and viscosity parameters $\alpha = 0.01$ (dotted curve), $\alpha = 0.1$ (smooth curve), and $\alpha = 0.4$ (dashed curve).

A.S. Klepnev and G. S. Bisnovatyi-Kogan

Astrophysics, Vol. 53, No. 3, p. 409-418, 2010

$$\tau_* = [(\tau_0 + \tau_\alpha)\ \tau_\alpha]^{1/2}$$

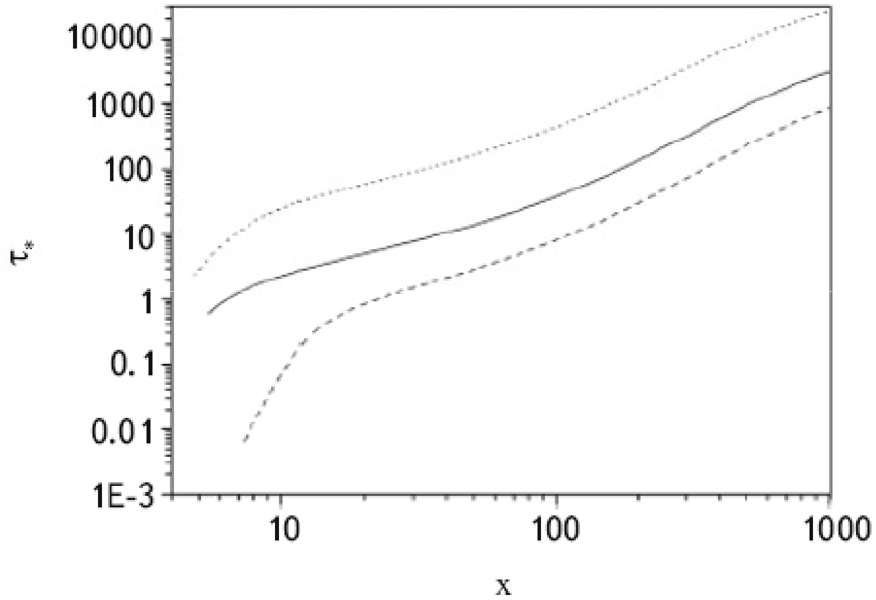

Fig. 2. The radial dependence of the effective optical depth of the accretion disk for an accretion rate $\dot{m} = 50$ and viscosity parameters $\alpha = 0.01$ (dotted curve), $\alpha = 0.1$ (smooth curve), and $\alpha = 0.4$ (dashed curve).

In Kerr metric BH the temperature in the optically thin region exceeds 500 keV – pair creation

W.A.Hiltner
ApJ, 1959

PHOTOELECTRIC POLARIZATION OBSERVATIONS OF THE JET IN M87*

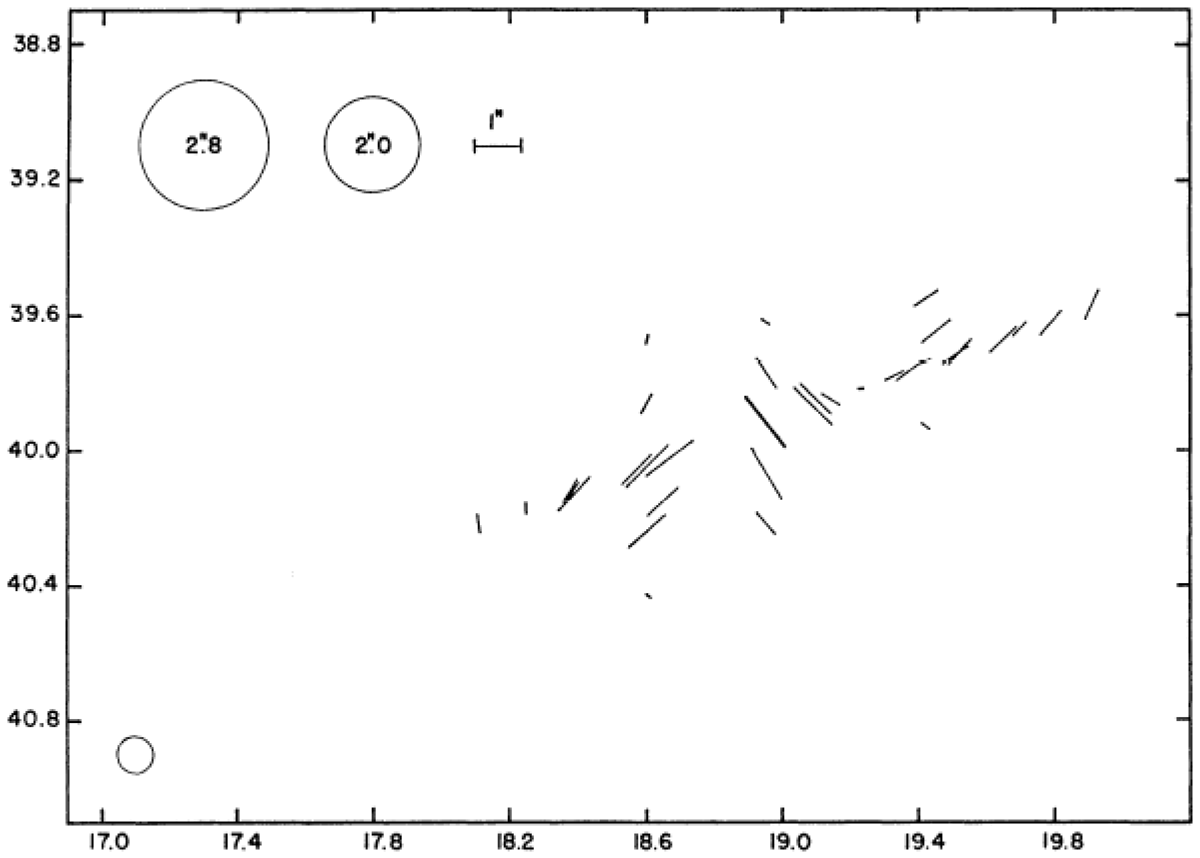

FIG. 1.—Polarization observations of M87. The co-ordinates refer to the observed position relative to a guide star. All lines refer to individual observations except the heavy one, which is the mean of ten observations. The relative sizes of the diaphragms used are shown in the upper left of the figure. The position of the nucleus of M87 is shown by a small open circle in the lower left.

Jet in M 87:

Radio: 6 cm (up
Optical: V-band
(middle),
Chandra:
X-ray 0.1-10 ke
(down)

Wilson , Yang
(2001)

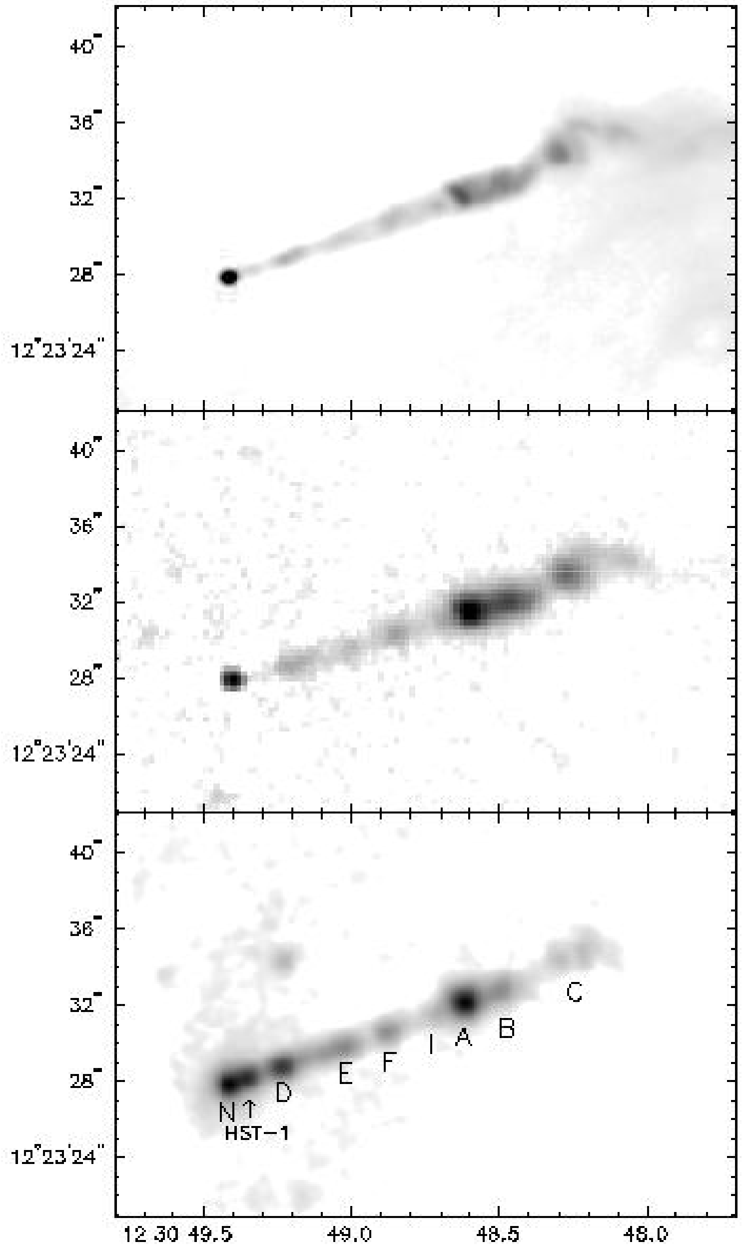

Magnetic jet collimation

jet as a capacitance-inductance system.

Sov. Astronomy, v.13, p. 369, 1969

A THEORY FOR THE FORMATION AND STABILITY OF THE JETS IN QUASARS AND RADIO-GALAXY NUCLEI

G. S. Bisnovatyi-Kogan, B. V. Komberg, and A. M. Fridman

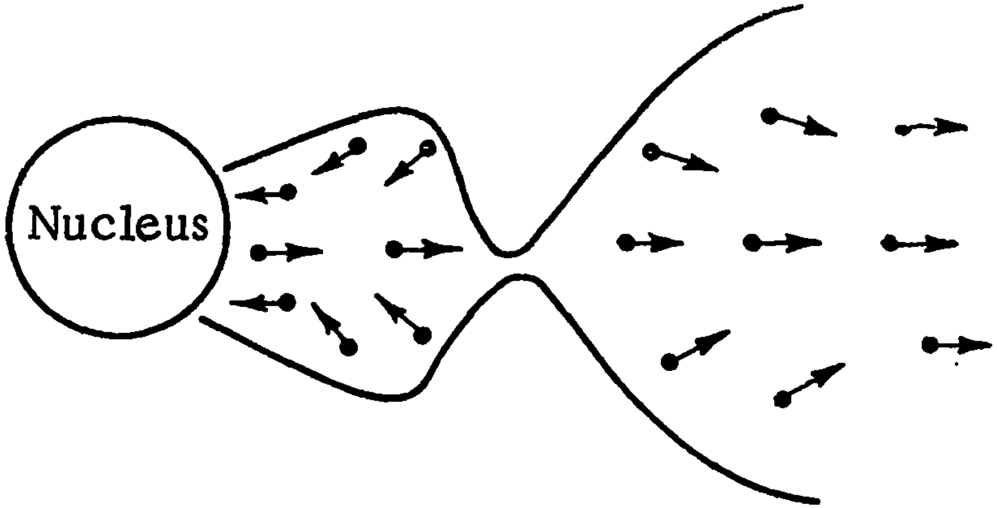

Oscillations with a period

$$T \sim \frac{L}{c}$$

Magnetic collimation is connected with torsional oscillations of a cylinder with elongated magnetic field.

We consider a cylinder with a periodically distributed initial rotation around the cylinder axis.

The stabilizing azimuthal magnetic field is created by torsional oscillations.

Approximate simplified model is developed. Ordinary differential equation is derived, and solved numerically, what gives a possibility to estimate quantitatively the range of parameters where jets may be stabilized by torsional oscillations.

Bisnovatyi-Kogan, MNRAS 376, 457 (2007)

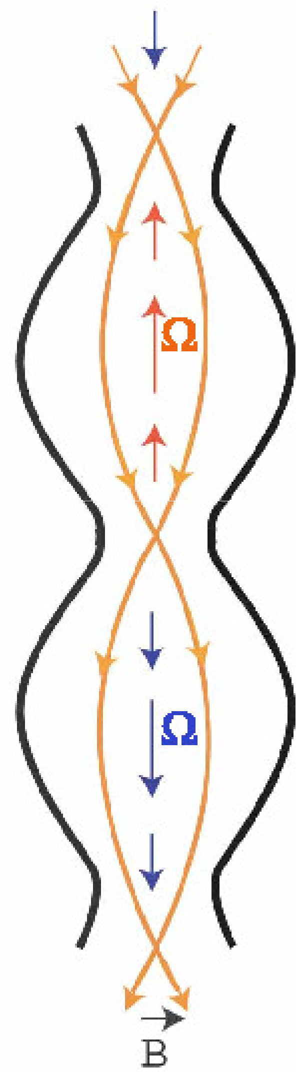
Ω
Ω
B

In non-dimensional variables differential equations have a form
(\tau – time; y- radius; z- radial velocity}

$$\frac{dy}{d\tau} = z, \quad \frac{dz}{d\tau} = \frac{1}{y}(1 - D\sin^2\tau); \quad y = 1,\ z = 0 \text{ at } \tau = 0.$$

Solutions for these initial conditions are obtained at different D
When y(0) is different from 1, there is a larger variety of solutions: regular and chaotic

$$D = \frac{1}{2\pi K C_m}\left(\frac{C_b \Omega_0}{z_0 \omega}\right)^2.$$

Frequency of oscillations \omega is taken from linear approximation (Alfven).
Angular amplitude \Omega is a free parameter.

Three possibilities

1. The oscillation amplitude is low (small D), so the cylinder suffers unlimited expansion (no confinement)

2. The oscillation amplitude is too high, so the pinch action of the toroidal fieeld destroys the cylinder, and leads to formation of separated blobs.

3. The oscillation amplitude is moderate, so the cylinder survives for an unlimited time, and its parameters (radius, density, magnetic field etc.) change periodically, or quasi-periodically in time.

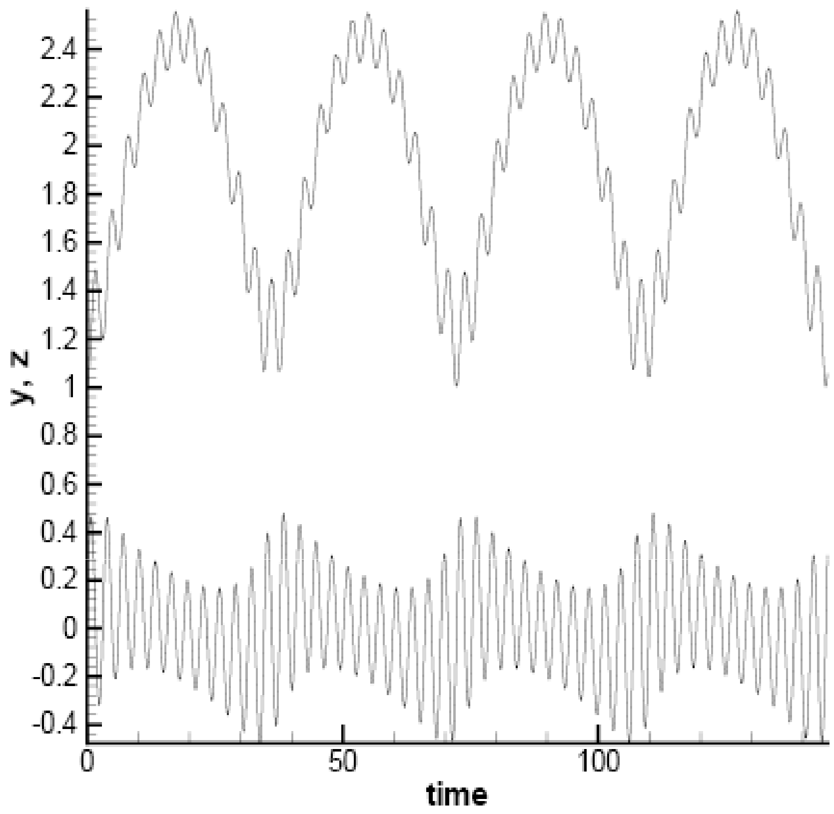

Figure 3: Time dependence of non-dimensional radius y (upper curve), and non-dimensional velocity z (lower curve), for $D = 2.1$.

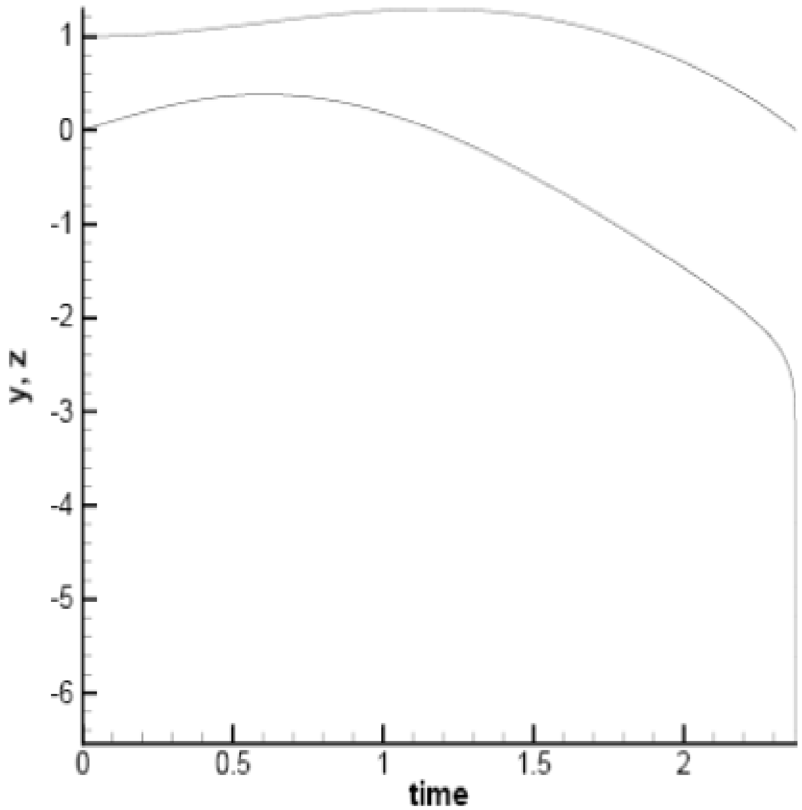

Figure 25: Time dependence of non-dimensional radius y (upper curve), and non-dimensional velocity z (lower curve), for $D = 3.1$.

The amplitude of torsion oscillations for collimation of the jet:

$$\Omega^2 R_0^2 = 2\pi^2 D \alpha_n^2 v_s^2 < c^2, \; R_0^2 = \frac{K}{\omega^2} = z_0^2 \frac{\rho_0 v_s^2}{\alpha_n^2 \pi B_{z0}^2}$$

This restrict sound velocity with the upper limit
v_s < c/2.

Such jet cannot be purely leptonic, and should contain barions

Development of chaos – Poincare sections

B.-K., A. Neishtadt, Z. Seidov , O. Tsupko .Yu. Krivosheev

(MNRAS, 2011)

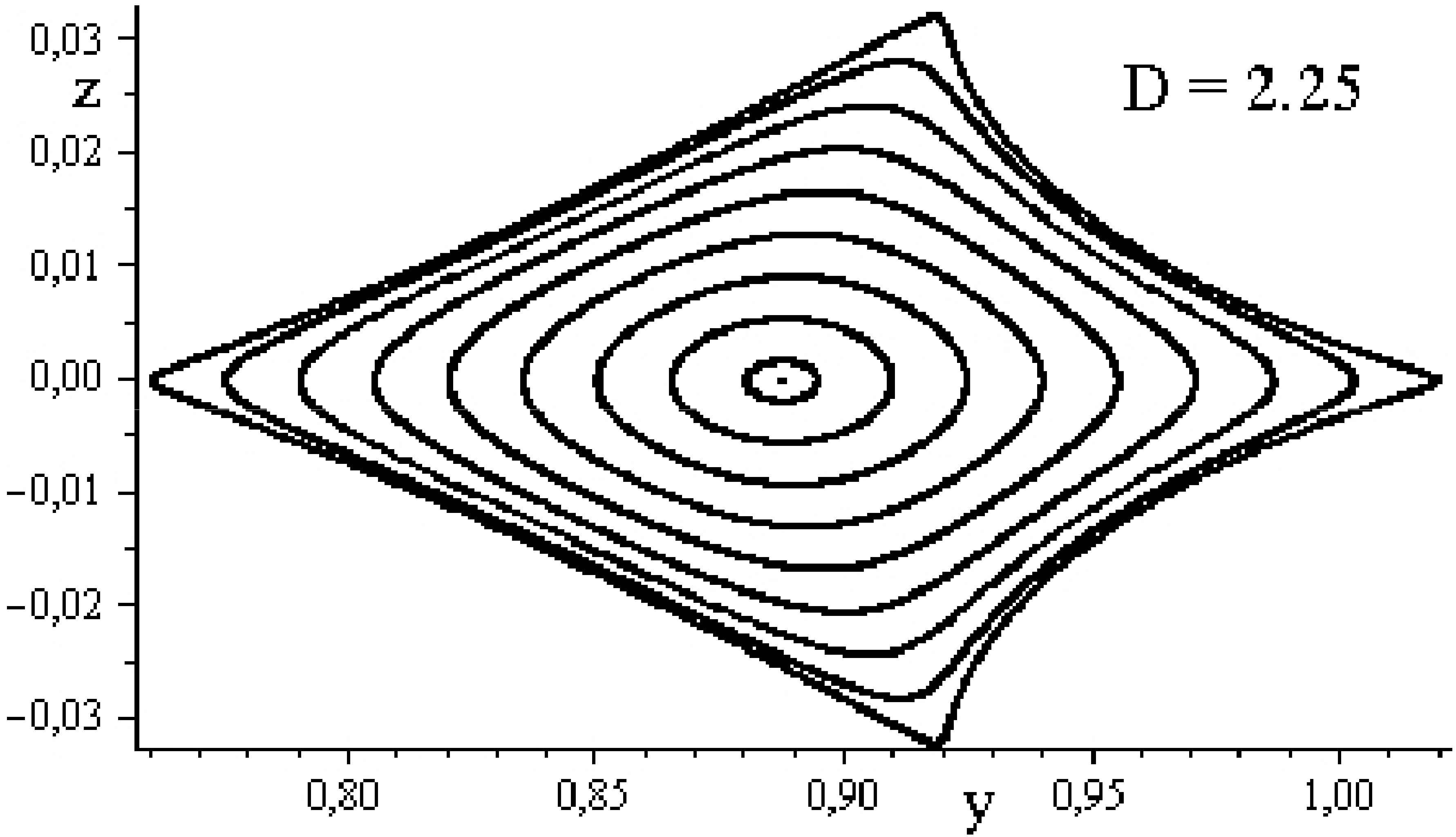

D = 2.25
z
y
0,03
0,02
0,01
0,00
−0,01
−0,02
−0,03
0,80
0,85
0,90
0,95
1,00

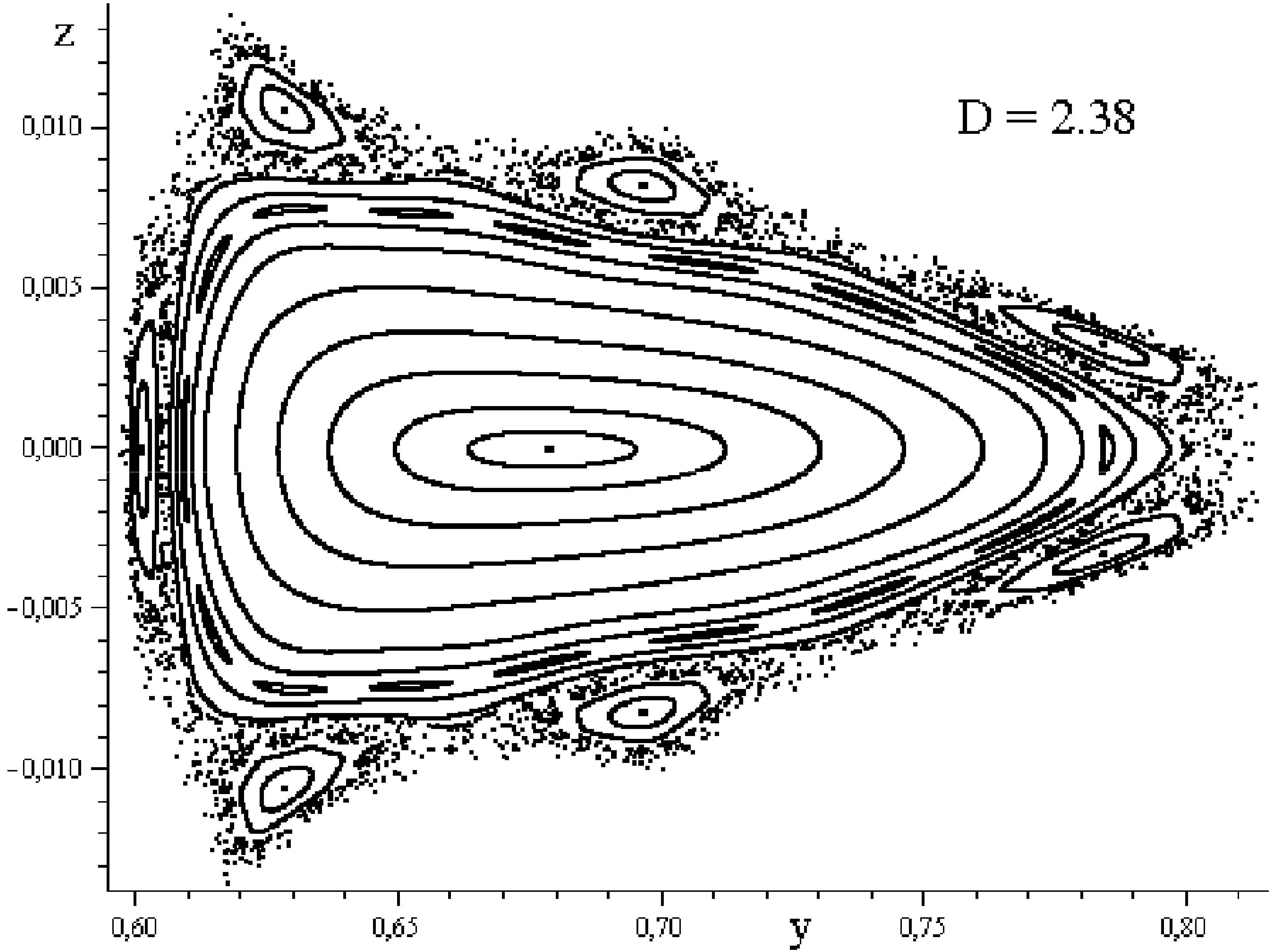
z
D = 2.38
0,010
0,005
0,000
-0,005
-0,010
0,60
0,65
0,70
0,75
0,80
y

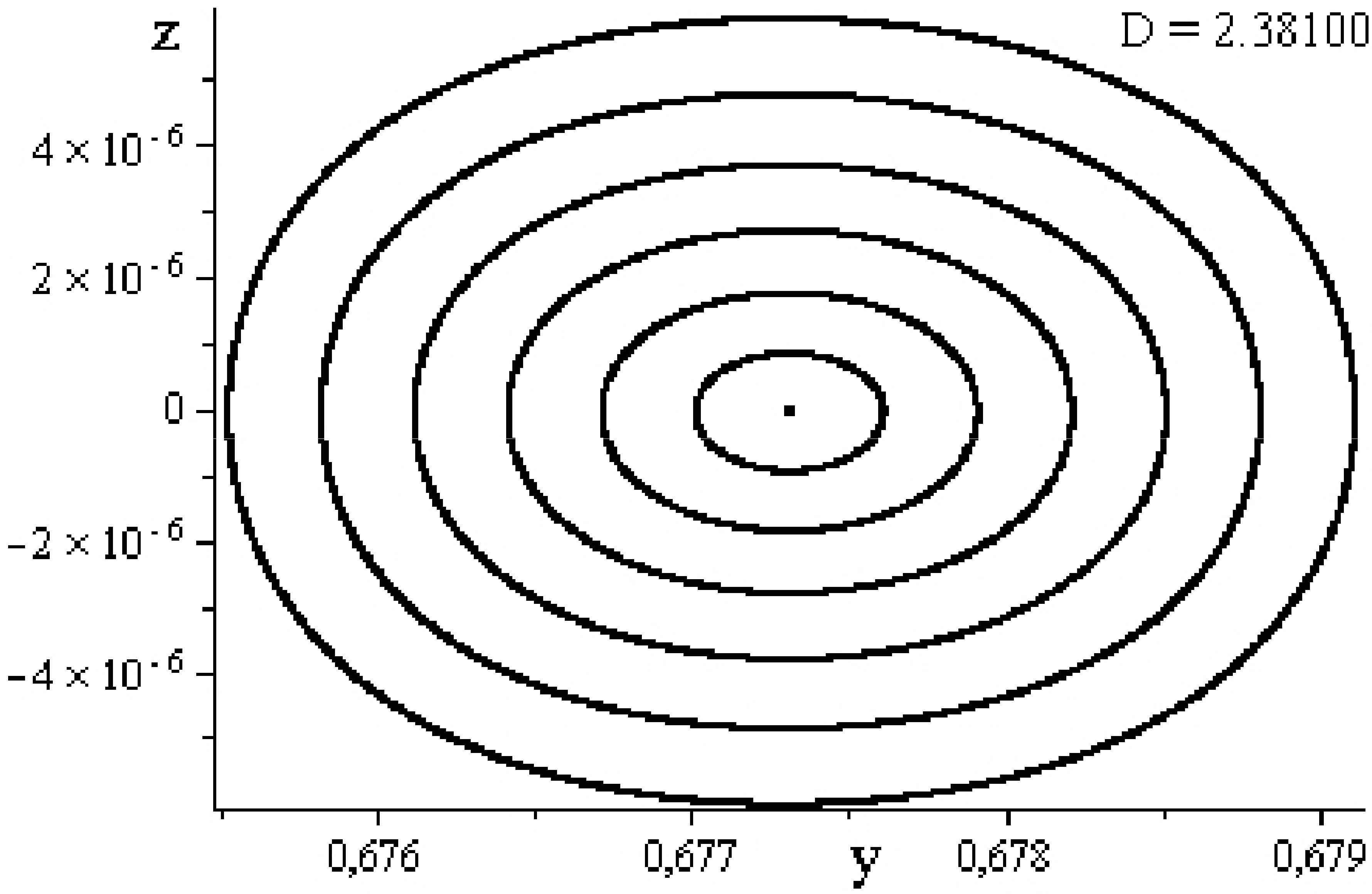
D = 2.38100
z
4×10^{-6}
2×10^{-6}
0
-2×10^{-6}
-4×10^{-6}
0,676
0,677
y
0,678
0,679

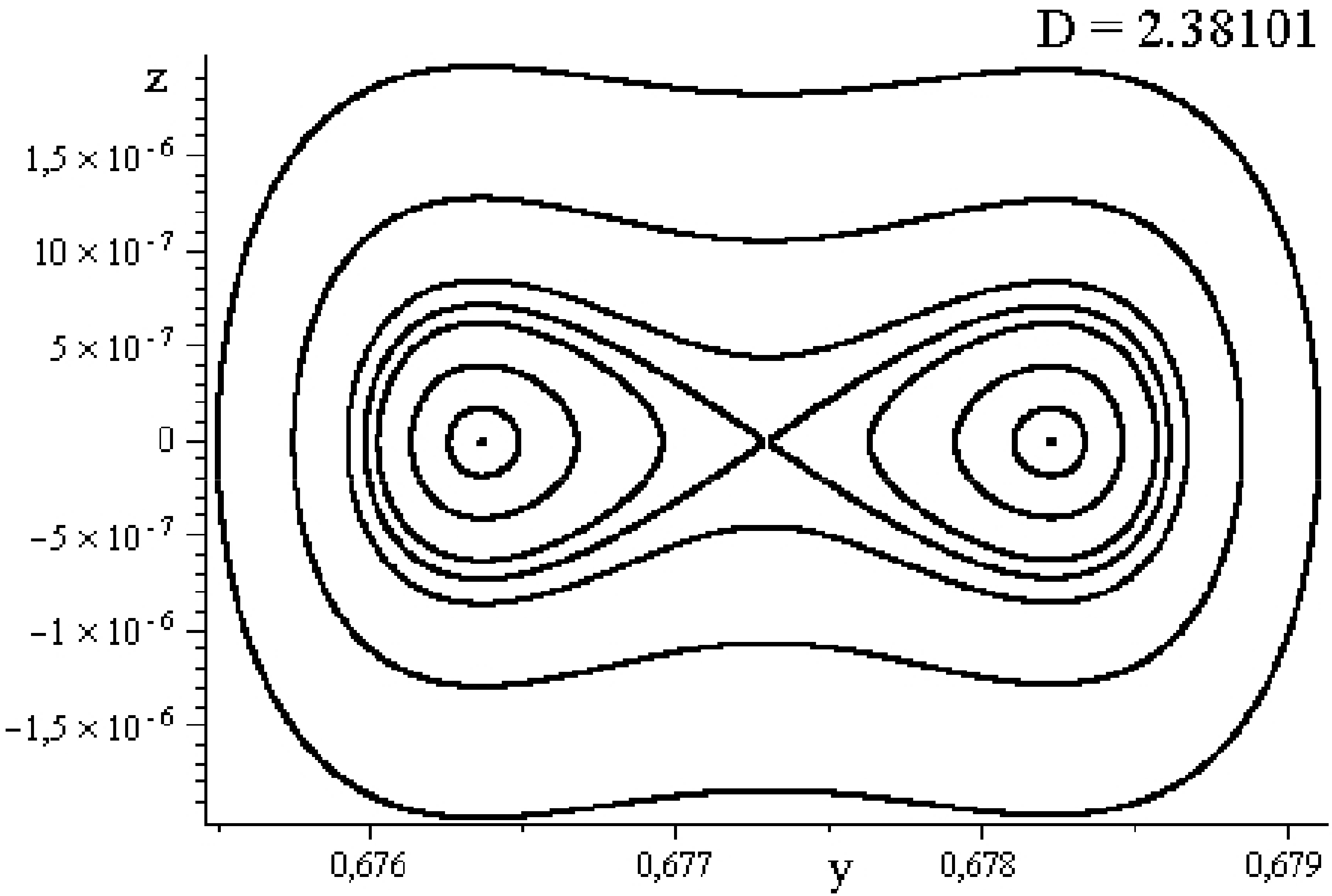

Feigenbaum sequence for the parameter D to reach the chaos

Numerical simulations of magnetized astrophysical jets in comnnection with laser-jet experiment NEODIM

V.S. Belyaev, G.S. Bisnovatyi-Kogan, A.I. Gromov, B.V. Zagreev, A.V. Lobanov, F.H. Matafonov, S.G. Moiseenko, O.D. Toropina

submitted

Similarity conditions

Laboratory jet after scaling   Jet in AGN nucleus (VLBI)

лабораторный джет после масштабирования	джет из АЯГ
$x = (0.3 \div 3) \times 10^{18}$ см	$3{\times}10^{18}$ см,
$t = 3 \times 10^{8}$ с	3×10^{10} см/с,
$v = 10^{9}$ см/с	3×10^{10} см/с,
$\rho = 10^{-26}$ г/см^3	10^{-26} г/см^3,
$n = 10^{-2}$ см$^{-3}$	10^{-2} см$^{-3}$,
$H = 10$–1 Гс	10^{-3} Гс,
$T = 10^{11}$ К	10^{11} К.

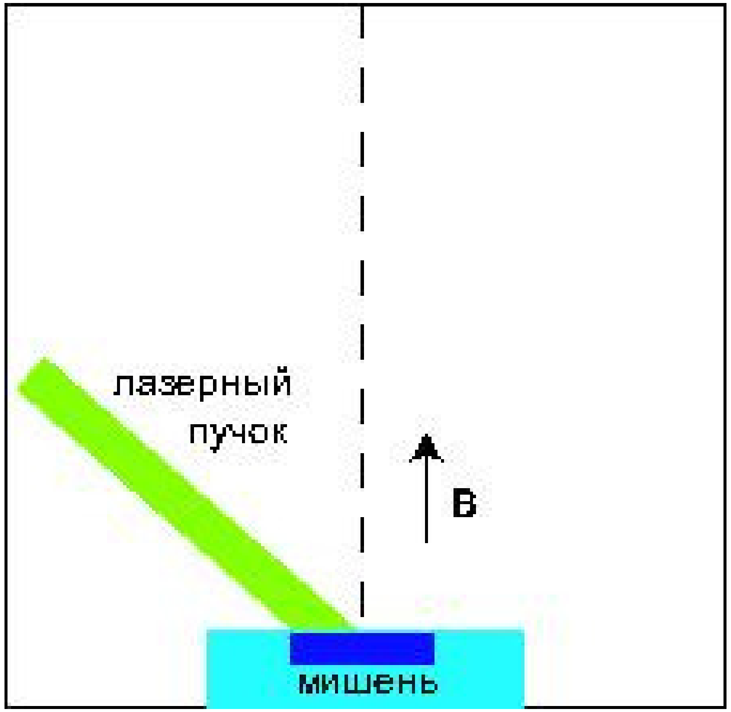

Scheme of the experiment

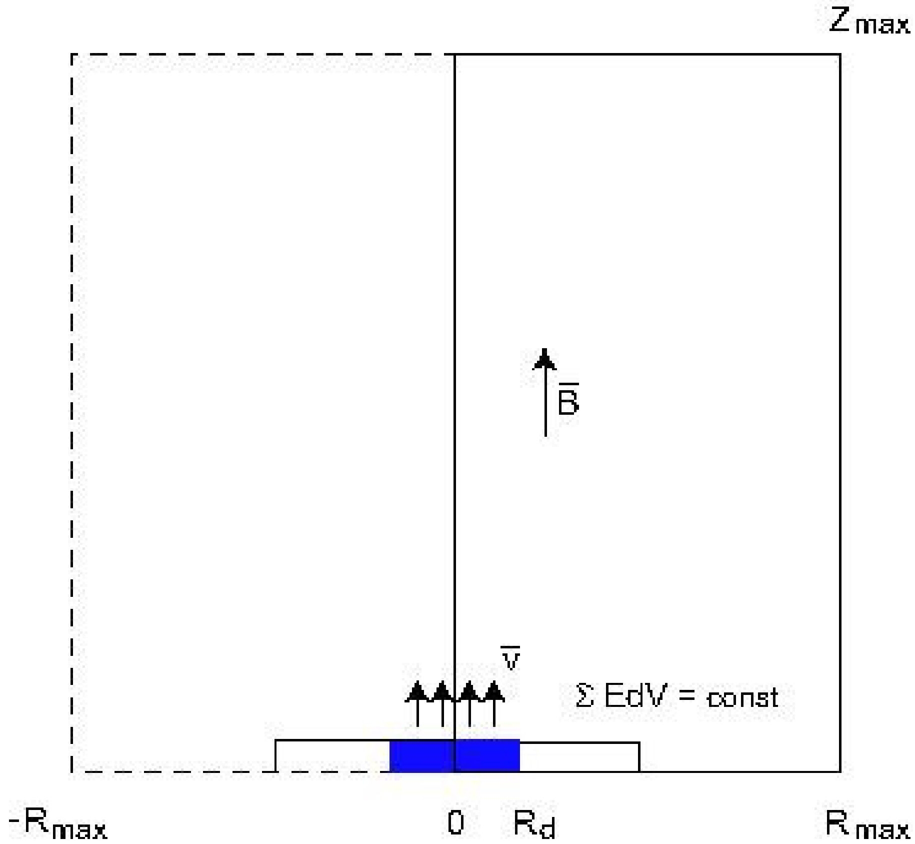

Numerical model

Non-ideal MHD equations, axial symmetry

$$\frac{\partial \rho}{\partial t} + \nabla \cdot (\rho\, \mathbf{v}) = 0\ ,$$

$$\rho \frac{\partial \mathbf{v}}{\partial t} + \rho(\mathbf{v} \cdot \nabla)\mathbf{v} = -\nabla p + \frac{1}{c}\mathbf{J} \times \mathbf{H}$$

$$\frac{\partial \mathbf{H}}{\partial t} = \nabla \times (\mathbf{v} \times \mathbf{H}) + \frac{c^2}{4\pi\sigma}\nabla^2 \mathbf{H}\ ,$$

$$\frac{\partial (\rho\varepsilon)}{\partial t} + \nabla \cdot (\rho\varepsilon\mathbf{v}) = -p\nabla \cdot \mathbf{v} + \frac{\mathbf{J}^2}{\sigma}\ ,$$

$$\frac{4\pi}{c}\mathbf{J} = \nabla \times \mathbf{H}\ . \qquad \mathbf{J} = \sigma(\mathbf{E} + \mathbf{v} \times \mathbf{H}/c)$$

$$p = (\gamma - 1)\rho\varepsilon \qquad \gamma = 5/3.$$

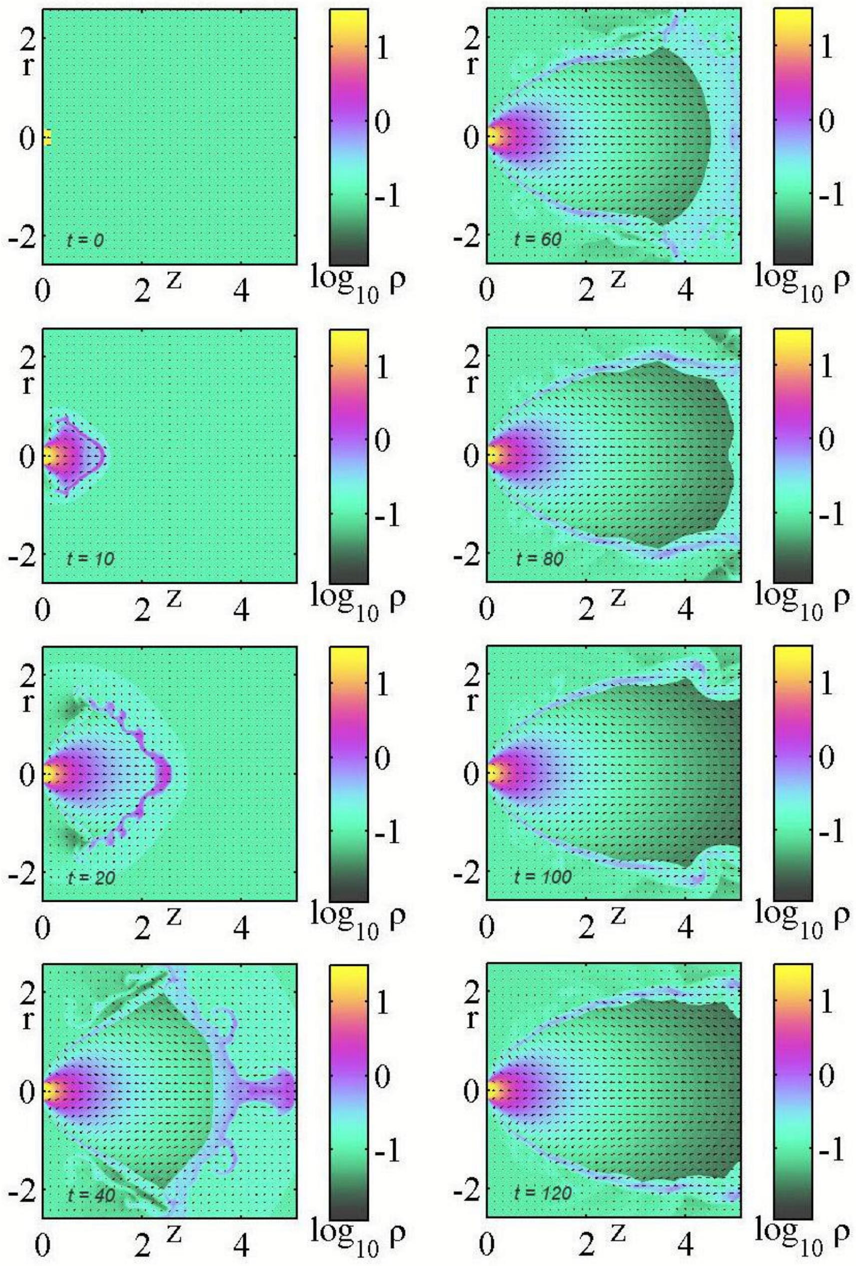

H=0

In the target

$\rho \approx 300\rho_0$

Supersonic injection

No collimation

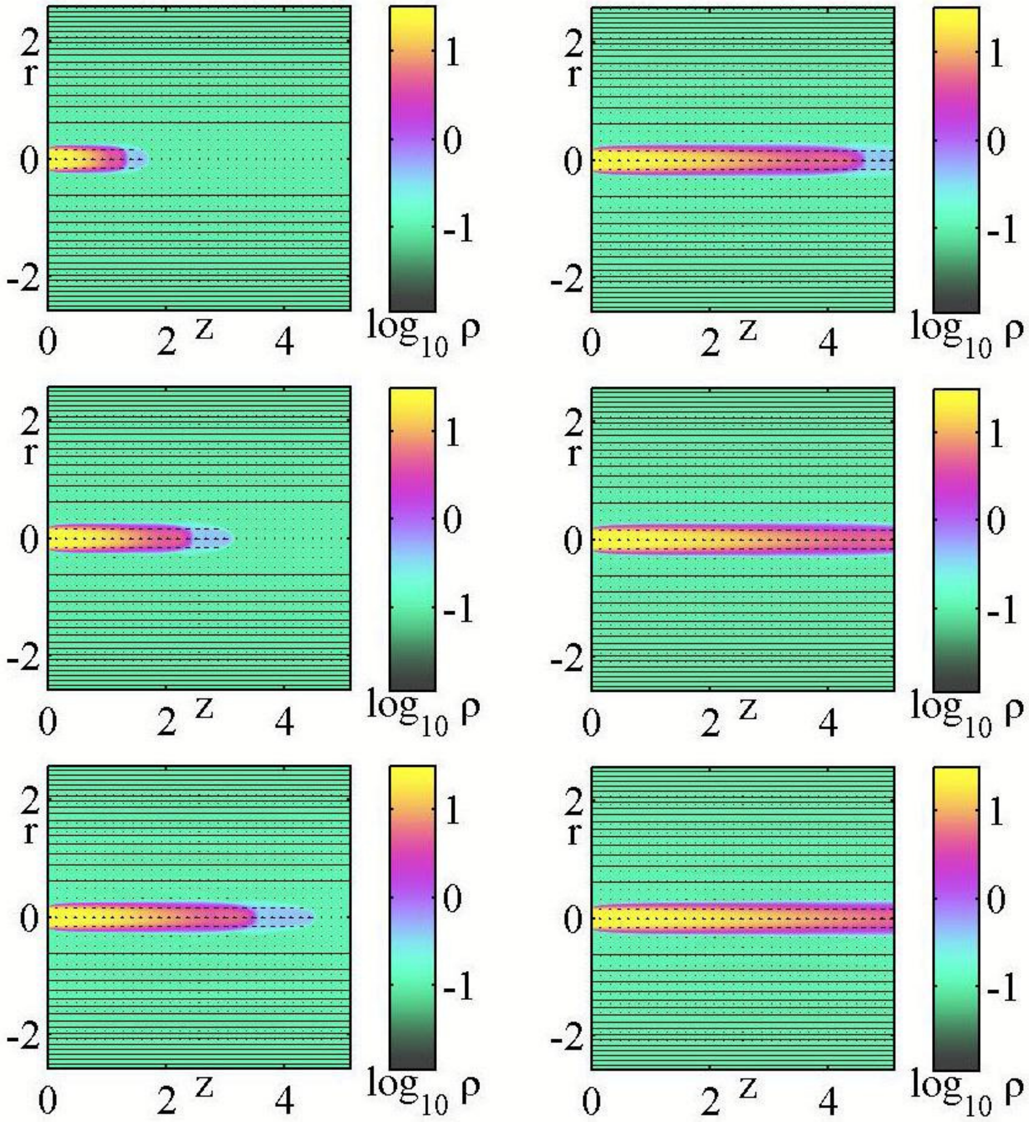

Poloidal magnetic field

$$\beta = \frac{8\pi P_\infty}{H_0^2} = 10^{-3}$$

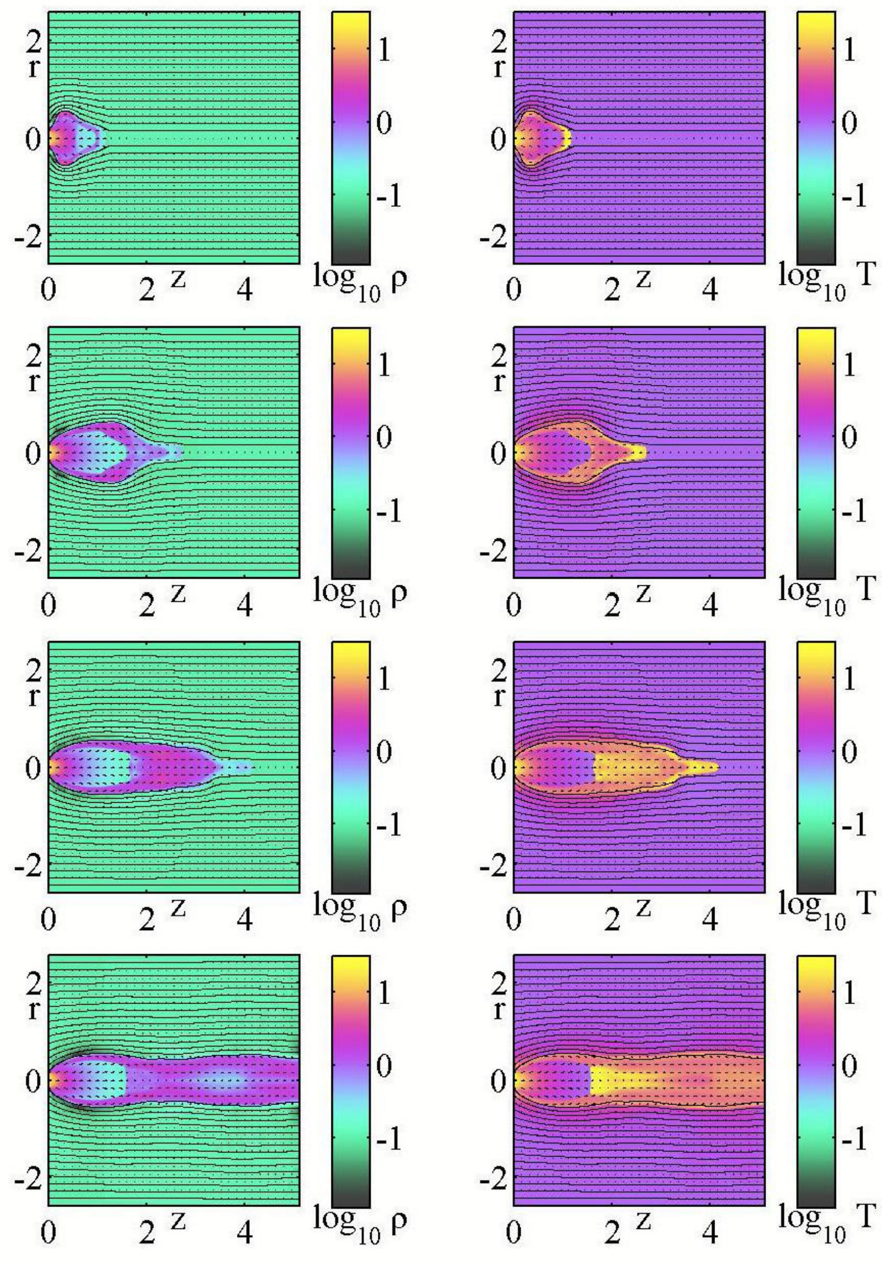

Poloidal magnetic field

$$\beta = \frac{8\pi P_\infty}{H_0^2} = 10^{-1}$$

Density - left column

Temperature - right column

Ring structure

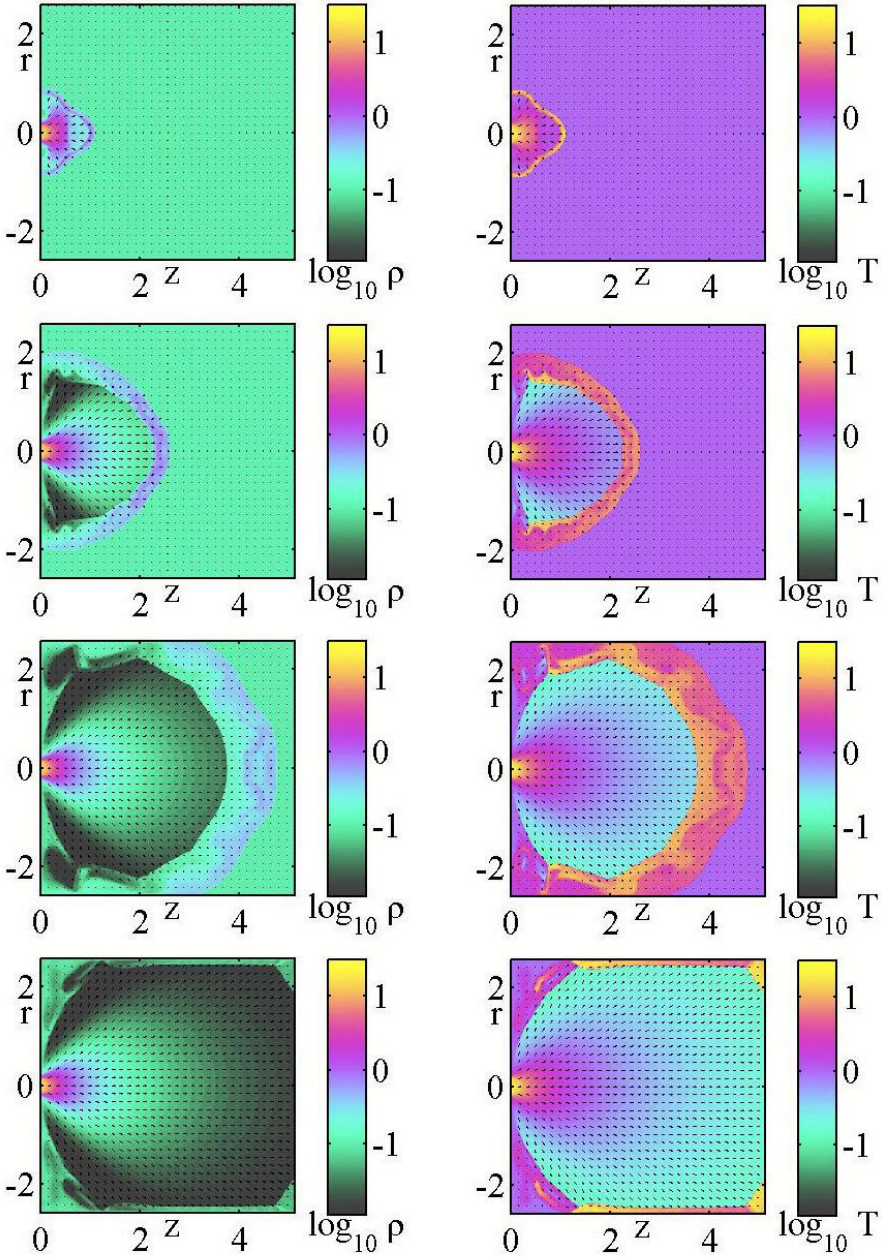

Toroidal magnetic field

$$\beta = \frac{8\pi P_\infty}{H_0^2} = 10^{-1}$$

$0 \le r \le R_d \quad H_\phi = H_0 r / R_d,$

$R_d \le r \le R_{max} \quad H_\phi = H_0 R_d / r$

R_d – target radius

No collimation

No rings

Magnetic field is too low

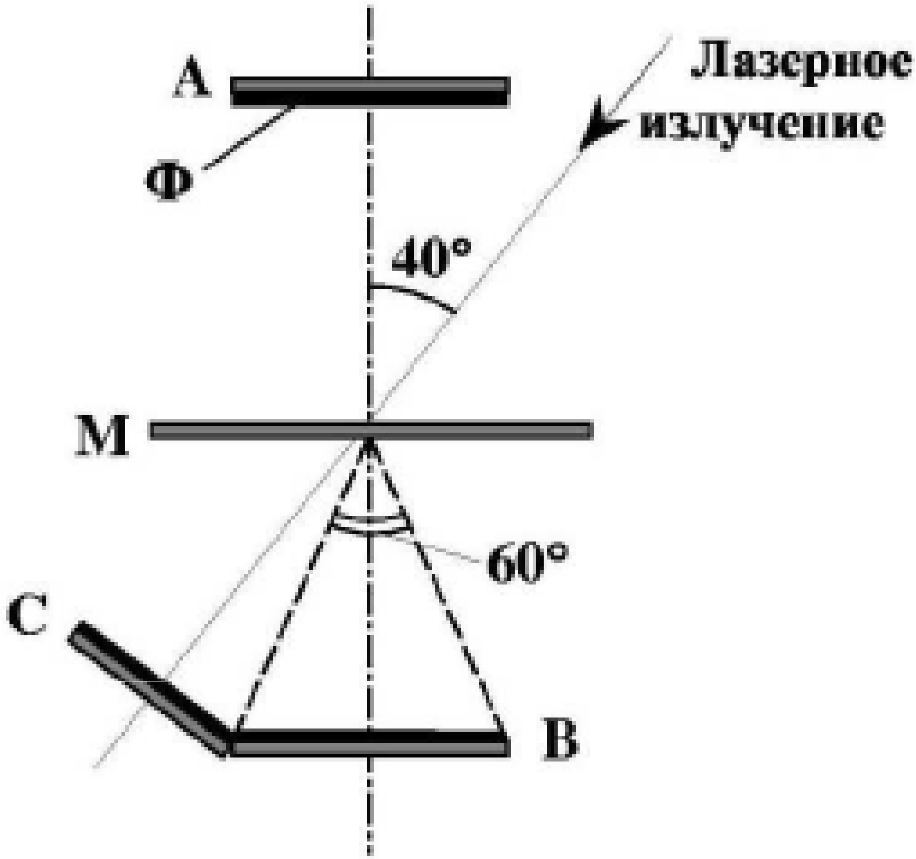

Experiment scheme

A,B,C – track detectors, Ф – Al filters,
M – Cu or Ta target

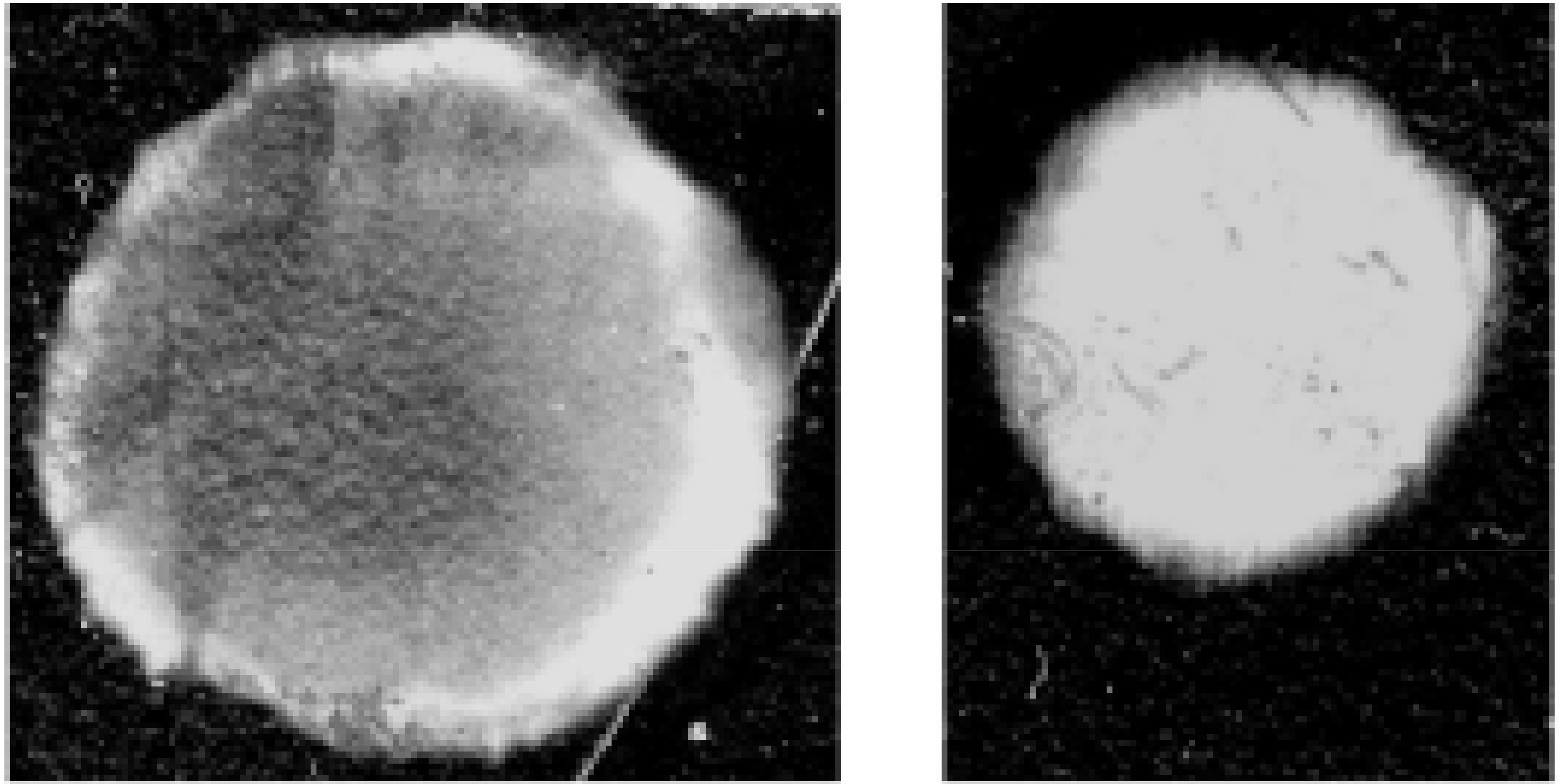

а $E_p > 0.8$ МэВ $\varphi_{1/2} = 21.8°$

б $E_p > 1.7$ МэВ $\varphi_{1/2} = 15.4°$

Proton beams at different energies

φ – proton deflection angle

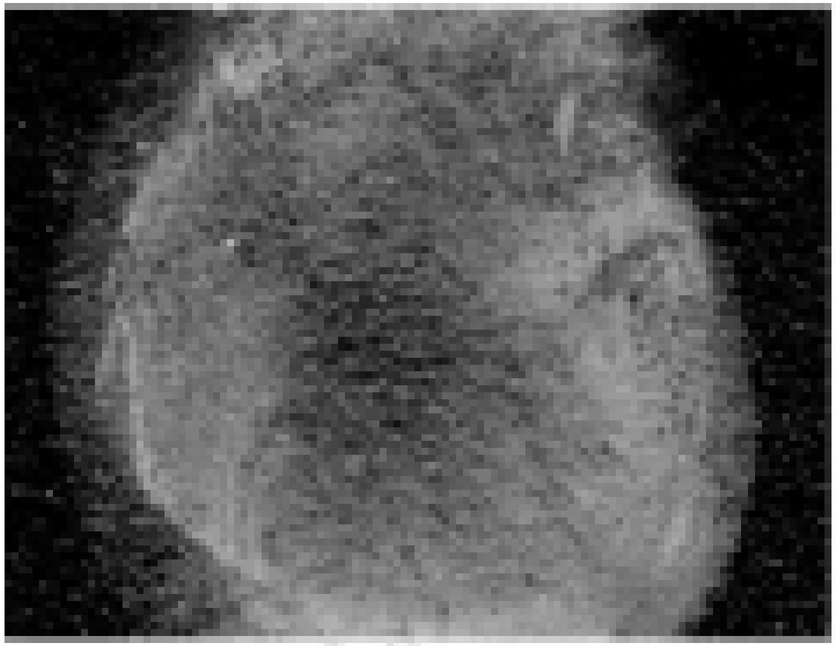

Cu 30 мкм

$\varphi_{0,5} = 20.5°$

Cu 50 мкм

$\varphi_{0,5} = 15.4°$

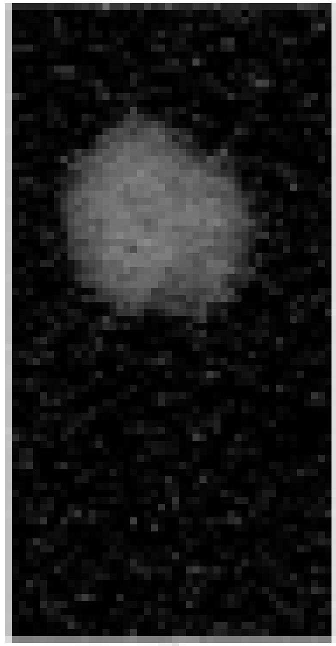

Ta 50 мкм

$\varphi_{0,5} = 5.7°$

Proton beams at same energy, different targets

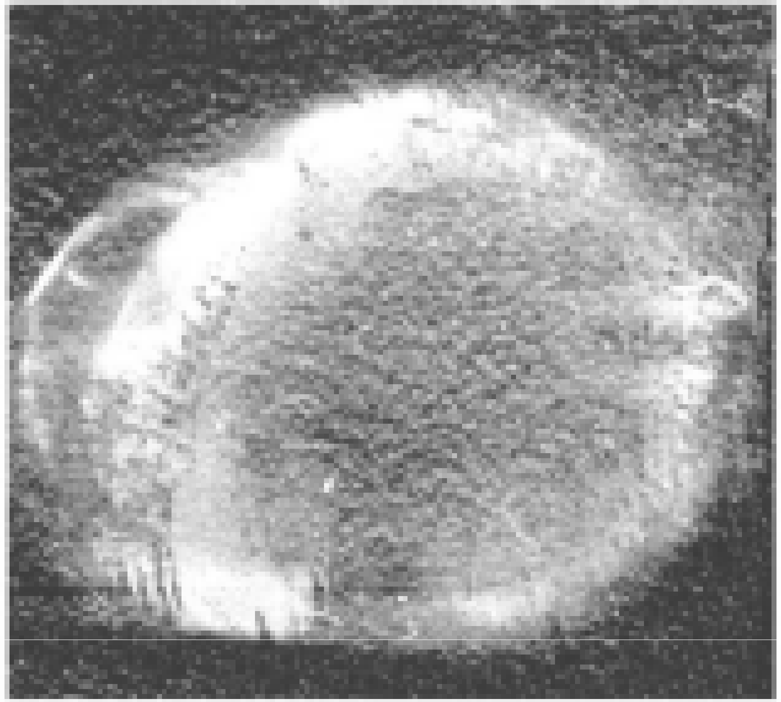

a $\varphi_{1/2} = 26.5°$

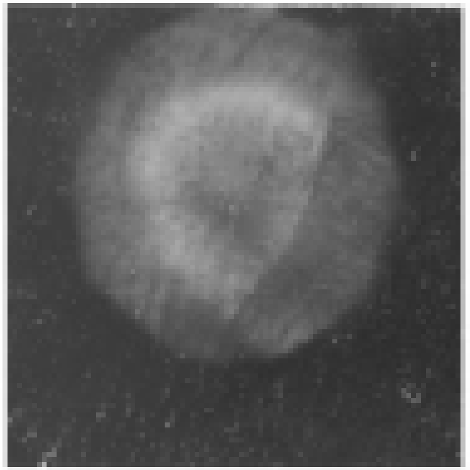

б $\varphi_{1/2} = 14°$

Proton beams at same energy, same target, different laser power $I = 2\times10^{18}$ (left), $I = 10^{18}$ (right) W/cm^2

Rings are visible in most pictures

Concluson - Problems

Jet origin (blobs or continuous injection; radiation pressure or explosions) BLOBS -?

Jet collimation (magnetic, or outer pressure, or kinematic)

Jet constitution (baryonic or leptonic) Baryonic -?

Particle acceleration (shocks, reconnection, kinetic)

Radiation mechanisms – (synchrotron, inverse Compton, nuclear processes)

Jets in Lab should help to answer!